ATMOSPHERIC SCIENCE

Toward practical stratospheric aerosol albedo modification: Solar-powered lofting

Ru-Shan Gao[1†], Karen H. Rosenlof[1*†], Bernd Kärcher[2], Simone Tilmes[3], Owen B. Toon[4], Christopher Maloney[1,5], Pengfei Yu[6*]

Many climate intervention (CI) methods have been proposed to offset greenhouse gas–induced global warming, but the practicalities regarding implementation have not received sufficient attention. Stratospheric aerosol injection (SAI) involves introducing large amounts of CI material well within the stratosphere to enhance the aerosol loading, thereby increasing reflection of solar radiation. We explore a delivery method termed solar-powered lofting (SPL) that uses solar energy to loft CI material injected at lower altitudes accessible by conventional aircraft. Particles that absorb solar radiation are dispersed with the CI material and heat the surrounding air. The heated air rises, carrying the CI material to the stratosphere. Global model simulations show that black carbon aerosol (10 microgram per cubic meter) is sufficient to quickly loft CI material well into the stratosphere. SPL could make SAI viable at present, is also more energy efficient, and disperses CI material faster than direct stratospheric injection.

INTRODUCTION

In the absence of mitigation, climate change by the end of this century is expected to produce severe and irreversible global impacts (*1*). A future with no substantial climate policy may see a warming of 3°C by 2100 (*1*). The Paris Agreement of the 21st Conference of the Parties to the UN Framework Convention on Climate Change (UNFCCC) aims to limit the increase in the global average temperature to well below 2°C above preindustrial levels and to pursue efforts to limit the temperature increase to 1.5°C. Global warming is likely to reach 1.5°C between 2030 and 2052, leading to irreversible loss of the most fragile ecosystems as well as substantial harm to the most vulnerable people and societies (*2*). Meeting the Paris Agreement limits requires rapid and far-reaching transitions in essentially all economic sectors. Immediate CO_2 emission reductions are needed to meet the 2°C Paris Agreement (*3*). If emission reductions are not achieved sufficiently fast, then the Paris temperature limits may be exceeded for years to decades and could be large enough to induce tipping points in the climate system. In this case, climate intervention (CI) methods may be implemented to avoid exceeding temperature limits ("flattening the curve") while necessary emission reductions and CO_2 removal efforts are conducted (*4*).

Various CI methods have been suggested to offset the warming caused by anthropogenic greenhouse gas emissions. Increasing Earth's albedo has been proposed as an effective means of reducing surface temperature increases (*5*–*8*). One extensively studied method to enhance Earth's albedo involves adding sunlight-reflecting aerosol to the stratosphere (stratospheric CI hereafter) (*6*, *9*, *10*). Other proposed methods include increasing the albedo of low-level clouds (*11*, *12*) and seeding cirrus clouds with ice nuclei (cirrus thinning) to allow more outgoing longwave radiation to escape to space (*13*, *14*).

Among these different methods, stratospheric CI has been identified as a potentially effective and affordable method for offsetting global warming caused by greenhouse gases (*8*). Implementing stratospheric CI requires injection of submicrometer-diameter aerosol particles or aerosol precursor gases into the stratosphere; modeling studies of this process have used altitudes well above the tropopause, at altitudes of 20 km or higher in the tropics. This method is associated with technical challenges and potential adverse effects (*5*, *8*, *15*) and thus is only considered as a temporary measure until greenhouse gas emission reductions occur. This present theoretical study explores a novel variation of stratospheric aerosol injection (SAI) that avoids development of new aircraft. The intent of this study is not to encourage SAI implementation but rather to provide the scientific foundation for societal decision-making regarding SAI.

The effectiveness of stratospheric CI has been postulated on the basis of observations and modeling results for the years following large volcanic eruptions. Moderate and large volcanic eruptions that result in large increases in stratospheric aerosol decrease surface temperatures for an extended period of time (*16*), demonstrating that, in principle, stratospheric CI is a viable technique. Although the effectiveness, potential benefits, and risks of stratospheric CI have not been studied extensively enough to thoroughly evaluate SAI proposals, even less effort has been put into the practical aspects of aerosol injection. Directly delivering aerosol material to altitudes of 20 km or higher at large rates [(≥teragram per year (Tg $year^{-1}$)] and dispersing the material poses serious technical challenges. Now, there are few aircraft or other platforms that can reach such altitudes and none with a suitably large payload capacity. A 2018 study (*17*) concluded that no capable aircraft exist and proposed the development of a new aircraft. Engineered particles that self-levitate photophoretically from an altitude of about 10 km have also been proposed (*18*). We note that none of these proposed technologies exist today.

In the summer of 2017, pyrocumulonimbus associated with extensive wildfires in the Pacific Northwest injected large quantities of

[1]National Oceanic and Atmospheric Administration Chemical Sciences Laboratory, Boulder, CO 80305, USA. [2]Insititut für Physik der Atmosphäre, DLR Oberpfaffenhofen, Wessling, Germany. [3]National Center for Atmospheric Research, Boulder, CO 80305, USA. [4]Department of Atmospheric and Oceanic Sciences, Laboratory for Atmospheric and Space Sciences, University of Colorado, Boulder, CO 80309, USA. [5]Cooperative Institute for Research in Environmental Sciences, University of Colorado, Boulder, CO 80309, USA. [6]Institute for Environmental and Climate Research, Jinan University, Guangzhou, China.
*Corresponding author. Email: karen.h.rosenlof@noaa.gov (K.H.R.); pengfei.yu@colorado.edu (P.Y.)
†These authors contributed equally to this work.

smoke into the Northern Hemisphere (NH) midlatitude stratosphere (*19*–*21*). This smoke, estimated to be 0.3 Tg of the carbonaceous aerosol mass with 2% black carbon (BC) and 98% organics, was lofted well into the stratosphere (up to 23 km) within 2 months of the initial injection at ~12 km and persisted for 9 months following the fires (*19*). The analysis of this event concluded that BC heating lofted the smoke-containing air parcels and suggests that BC could be used to intentionally loft selected aerosol materials to altitudes suitable for CI. In addition, we note that the pyrocumulonimbus injection altitude of 12 km is readily accessible by existing commercial aircraft.

On the basis of our knowledge of the 2017 fire case, we explore solar-powered lofting (SPL) as a means to transport CI material (CIM), such as noncondensing gases (e.g., SO_2) or engineered particles, from an initial, much lower-altitude injection site to well within the stratosphere. Specifically, particles that absorb solar radiation (hereafter called radiation-absorbing particles or RAP) heat the surrounding air that then rises, lofting the CIM to stratospheric altitudes. In contrast to proposed techniques that require airborne platforms to reach 20 km for injection of CIM, SPL substantially reduces the platform energy requirements and eliminates the need to develop new specialized stratospheric aircraft.

In evaluating SPL here, BC is used as an example RAP. With the addition of RAP, minimizing stratospheric warming becomes an important requirement. For example, a modeling scenario using 1 Tg $year^{-1}$ of BC produced a stratospheric warming of 60°C (*22*). Large stratospheric heating was also modeled for 5 Tg of BC injected from a regional nuclear exchange that produced surface cooling (*23*). As discussed below, BC quantities proposed here for SPL are much smaller than for those extreme cases.

RESULTS

SPL modeling

The National Center for Atmospheric Research (NCAR) Community Earth System Model (CESM) with the Community Aerosol and Radiation Model for Atmospheres (CARMA) aerosol package (*24*) is used to simulate SPL and calculate the amount of BC required to achieve equivalent effectiveness as for the stratospheric injection case. The lofting rate depends solely on the concentration of BC; so to simulate the relevant process, one grid cell is filled with a specified concentration of BC. This method allows an estimation of the lowest BC concentration that lofts most of the CIM injected at achievable altitudes for conventional heavy-lift aircraft (~13.5 km) to a stratospheric altitude of 20 km. While the CESM climate model provides a global view, its spatial resolution (grid size of 208 km by 279 km) is too coarse to resolve plumes injected by individual aircraft. A Gaussian diffusion model is then used to determine the total amount of BC injected by a number of discrete plumes that is required on a yearly basis for a nominal SO_2 injection scenario (see Materials and Methods).

The injection of a sufficient amount of BC at 13.5 km at any latitude allows ascent into the stratosphere; this was clear based on observations from the 2017 Pacific Northwest fire event where the injection latitude was in a climatological descent region in the stratosphere. However, SPL with injection altitude in the troposphere will be most effective at latitudes where air is typically rising, such as in the upward branch of the Hadley cell (and Brewer-Dobson circulation) nominally between ±30° latitude. This region is broad enough to accommodate multipoint injection schemes used in previous modeling studies (*25*).

The modeled effectiveness of SPL is gauged relative to injections at 20 km, a hypothetical injection level used in prior modeling work. In the simulations, 2 Tg of SO_2 (1 Tg of sulfur) is used as the CIM. Once in the stratosphere, SO_2 coverts to sulfate aerosol, and the total amount of sulfur and its gas-to-aerosol partitioning is tracked. The mass of sulfate aerosol from a 20-km injection without BC and a 13.5-km injection with BC are compared. To simulate a scenario that is realistically achievable, the lower altitude injection is performed over a single 10-day period and repeated annually. Details are given in Materials and Methods.

To demonstrate SPL, the equatorial injections done over a 10-day period every June are presented. It is not the ratio of BC to SO_2 that is important for the lofting but rather the ratio of BC to total air mass at the injection altitude. The 2 Tg $year^{-1}$ of SO_2 used here is on the low end of the proposals to keep surface warming below 2°C in 2100 (*26*) and is comparable with that needed for the current decade assuming the Representative Concentration Pathway (RCP) 8.5 scenario. Any amount of coinjected SO_2 is possible up to the limits imposed by the aircraft deployed and the molecular number density of air at flight altitude.

Figure 1A shows the results from three simulations using 2 Tg of SO_2 as the CIM. In the first simulation, SO_2 was injected into one model grid box at 13.5 km; in the second, SO_2 was injected at 20 km; and in the third, SO_2 plus BC with a concentration of 10 μg m^{-3} was injected at 13.5 km. In the first case, virtually, no sulfate aerosol is formed in the stratosphere. In the second case, about 90% of the injected sulfur is present in the stratosphere as sulfate aerosol within a month. The sulfate aerosol loading gradually decreases until the next injection of the following year. Over the course of a year, approximately half of the injected sulfur is lost through both particle sedimentation and transport by the downward branch of the Brewer-Dobson circulation. In the third case, the amount of stratospheric sulfate aerosol slightly exceeds that for the direct injection at 20 km (second case), demonstrating the fundamental effectiveness of SPL. If the injection altitude is increased to 14.5 km, then the amount of BC required to achieve the same aerosol loading is reduced by 20%. Figure 1B displays the sulfate aerosol distribution as a function of latitude. The burdens in the Northern and Southern Hemispheres are similar, with half of the aerosol in the 30°N to 30°S band. Injections off the equator or in different seasons will produce a different partitioning between the hemispheres. The injection latitude could be adjusted to maximize surface cooling where needed.

A BC concentration of 10 μg m^{-3} produces rapid lofting. To demonstrate the rate of lofting, a passive tracer along with the BC was injected in one grid box at 13.5 km on the fifth day of our 10-day injection. Figure 2 shows the vertical profiles of the resultant tracer mixing ratios. The peak concentration reaches the tropopause, at 16.5 km, in 3 hours. Within 2 days, there is material lofted well into the stratosphere. A complementary run with the same amount of passive tracer but no BC exhibits essentially no change in the altitude of the passive tracer peak over the 48-hour simulation.

SPL implementation

SPL implementation requires aircraft to disperse RAP and CIM in a volume of air at the chosen lofting location over a fixed period of time. Multiple aircraft create plumes of these materials over the

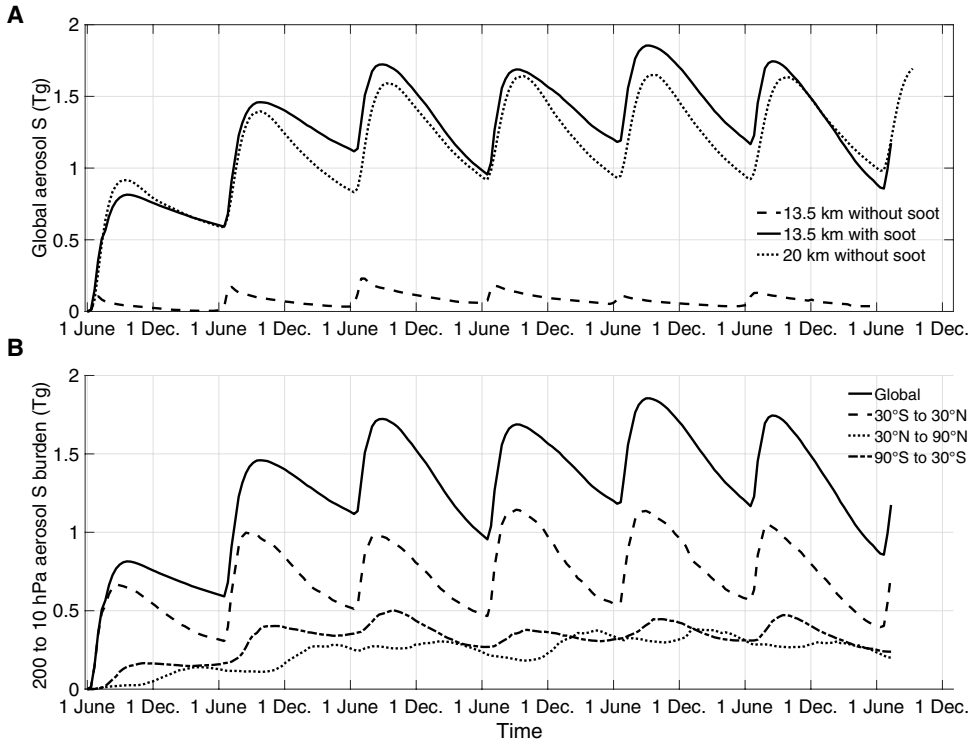

Fig. 1. Sulfate aerosol burden in the stratosphere. The burden is summed from 200 hPa to the model top at 10 hPa. (**A**) Burden remaining from a 2 Tg year^{-1} of SO_2 injection at 20 km (dotted line), at 13.5 km (dashed line), and at 13.5 km including BC (solid line). For each scenario, the injection was over a 10-day period every June at the equator. (**B**) Burden for the injection at 13.5 km including BC in latitude bands: Solid line is global, dashed line is 30°N to 30°S, dotted line is 30°N to 90°N, and dash-dotted line is 30°S to 90°S. The model is running in a free mode, so there is natural variability in the dynamics impacting the aerosol loading from year to year. It takes approximately 2 years to reach a pseudo equilibrium loading, and interannual variability is apparent in the last 4 years plotted.

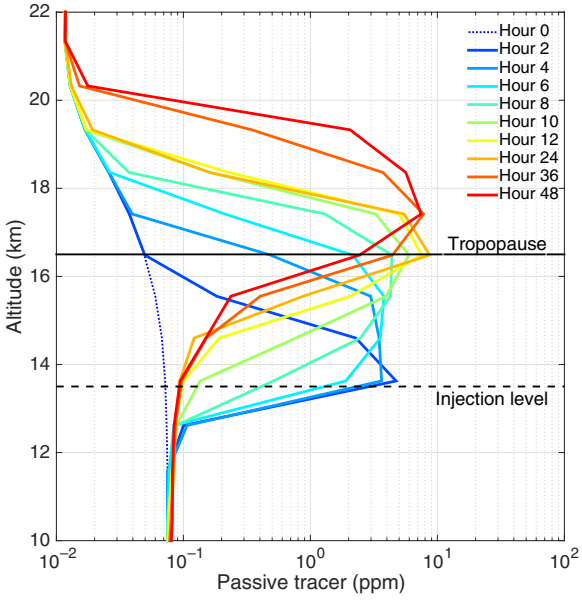

Fig. 2. Evolution of a pulse injection of a passive tracer. This is for the model case with BC (10 μg m^{-3}) injected at 13.5 km. The colored lines show zonally averaged (from 20°S to 20°N) tracer mass mixing ratio from the start of the injection to 48 hours after injection. ppm, parts per million.

same length of flight track and within a much narrower horizontal distance than the flight track length. The RAP accumulates in the flight region, eventually reaching the critical concentrations for lofting.

A plume, once created in the troposphere from an aircraft, disperses through turbulent mixing and diffusion, which reduce the initial RAP concentration. To calculate the initial concentration of BC required to achieve lofting, a two-dimensional Gaussian plume model (*27*) is used to estimate the dispersion in a vertical plane that is perpendicular to the plume length (cross-sectional dispersion). Dispersion along the plume length is not considered on the basis of the assumption that the plume length is much larger than the dispersion distance. The Gaussian model is controlled by vertical and horizontal diffusion coefficients and vertical wind shear. These parameters are based on previous work (*28*) using large-eddy simulations to derive a range of vertical and horizontal diffusion coefficients consistent with in situ observations (*29*). Maximum values of vertical and horizontal diffusion coefficients (23 and 0.6 m^2 s^{-1}) and vertical wind shear (0.007 s^{-1}) (*27*, *28*) are used here to estimate the upper limits of plume dispersion and thus the upper limit of the required BC. Multiple plumes within the chosen width of the injection volume are then combined to determine the three-dimensional distribution of materials for a 10-day injection event (see Materials and Methods).

The plume modeling results indicate that an 8-km width is sufficiently wide for the injection area to limit the effect of plume dispersion. In this case, an initial BC concentration of 1.4 times the value

derived for uniform distribution in a CESM model grid box will be sufficient to loft the CIM into the stratosphere (see Materials and Methods). The length of the injection area is chosen to be 100 km. Assuming this configuration, the amount of BC required over the 10-day injection period is 10 Gg (see Materials and Methods). This value is an upper limit because of the upper limit diffusion coefficients used in this work.

A large number of aircraft are needed to deliver the required BC and CIM mass in a 10-day period. A large aircraft with the size of a military tanker or a Boeing 747 carries on the order of 10^5 kg (~100 m^3 of liquid SO_2). Therefore, delivering 2 Tg requires about 20,000 flights. Assuming 2 hours per flight, the injection can be done over a one 10-day period using 335 aircraft, with each aircraft flying during daylight hours six times per day. Short flights allow increased payload because the required fuel load will be less than maximum.

Accommodating 20,000 flights in 10 days requires using at least eight runways simultaneously. This requirement can be met with two large airports separated by ~200 km or less. For perspective, 2 Tg is approximately 20% of the annual enplaned international cargo (Bureau of Transportation Statistics, transtats.bts.gov). The nominal CO_2 emissions increase due to 40,000 flight hours of a Boeing 747 is a small fraction of the annual global aviation emissions. Assuming an emission rate of approximately 90 kg CO_2 $hour^{-1}$ for a Boeing 747 at cruise, the injection results in an increase over the 2018 global aviation emissions of 0.0004%. Injection could also be done over a longer period or multiple periods per year with fewer aircraft but would result in a larger amount of BC emitted annually. Injected CIM mass, and hence number of flights, is halved if H_2S or pure sulfur (oxidized in situ) is used instead of SO_2 (*30*).

The present study does not address all the technological issues unique to SPL that require consideration before implementation. For example, a determination as how best to disperse solid BC with gaseous/liquid SO_2 or solid particles such as Al_2O_3 from an aircraft is needed. Research is also needed to find the best light-absorbing material for SPL, the optimal size distribution to maximize heating per unit mass, and the means to achieve that size in the injection process. Whether there are interactions between BC aerosol and the gaseous or aerosol CIM needs to be assessed via laboratory and field experiments. Although the time scale of lofting is short, SO_2 oxidation while the air is rising needs to be examined in detail. Work is also required to determine the maximum amount of CIM that can be lofted through this approach.

More theoretical study is required to optimize aircraft deployment locations, injection locations, and preferred seasons to best achieve the desired mitigation outcomes; this applies to SAI by both direct injection and SPL. Here, we discuss one possible scenario, injection only in June and on the equator. For direct injection, latitudes and seasons of injection have been explored (*31*) at altitudes 5 km above the tropopause. Injecting during one season was found to reduce the amount of SO_2 needed to achieve a certain aerosol optical depth when compared to injecting the same amount over an entire year, possibly minimizing side effects. Injections slightly off the equator may also be more effective (*31*). Whether SO_2 is the best CIM to use also requires investigation. There may be other particulates that minimize side effects, and laboratory work along with modeling is needed for those investigations.

Using solar energy to achieve stratospheric injection in the SPL method has distinct advantages over direct injection SAI. With injection in the upper troposphere, SPL circumvents the need to develop a new airborne platform for injecting CIM directly into the stratosphere. Injection in the upper troposphere will also require less fuel than introducing the same mass at higher altitudes and hence is likely to be more cost effective. Another advantage of injecting material in the troposphere is that CIM is better dispersed than if directly injected by similar methods in the thermodynamically stable stratosphere. Evidence of limited stratospheric dispersion derives from the chance encounter of a high-altitude research aircraft with a well-defined stratospheric rocket plume that occurred over California more than 10 days after the rocket launch from Kazakhstan

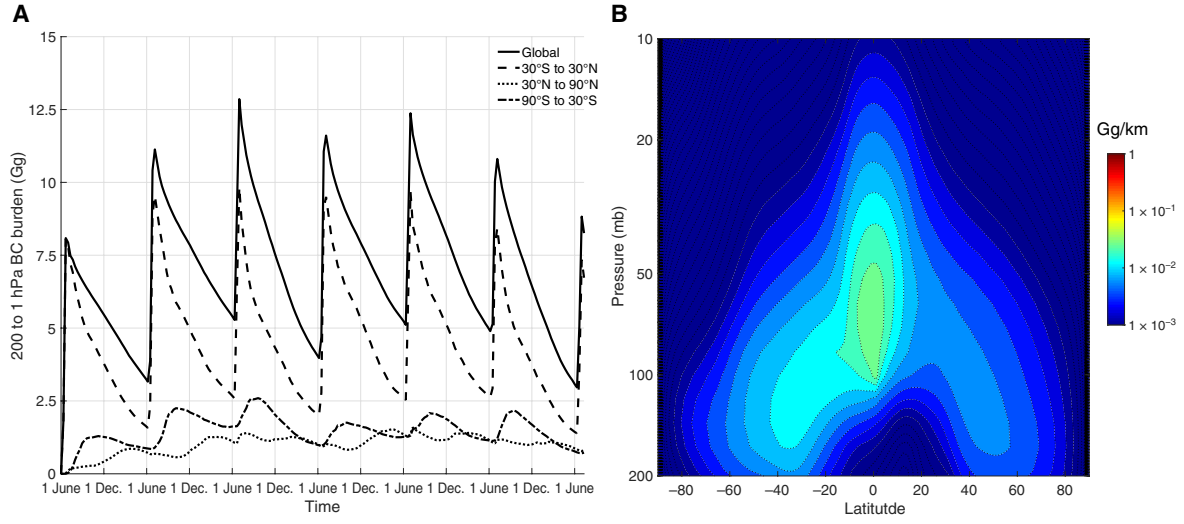

Fig. 3. BC burden as a function of time and annual average contribution (in concentration) for the SPL scenario. (**A**) BC aerosol burden (summed from 200 to 1 hPa) remaining from a tropical 10-Gg injection over 10 days every June. Solid line is the global burden, dashed line is the tropical burden, dotted line is the NH 30°N to 90°N burden, and dash-dotted line is the Southern Hemisphere 30°S to 90°S burden. (**B**) Annual average difference in BC concentration (gigagram/kilometer) between a case with no BC added and a case with BC of 10 Gg $year^{-1}$ [average of 3 to 6 years from the run shown in (A)].

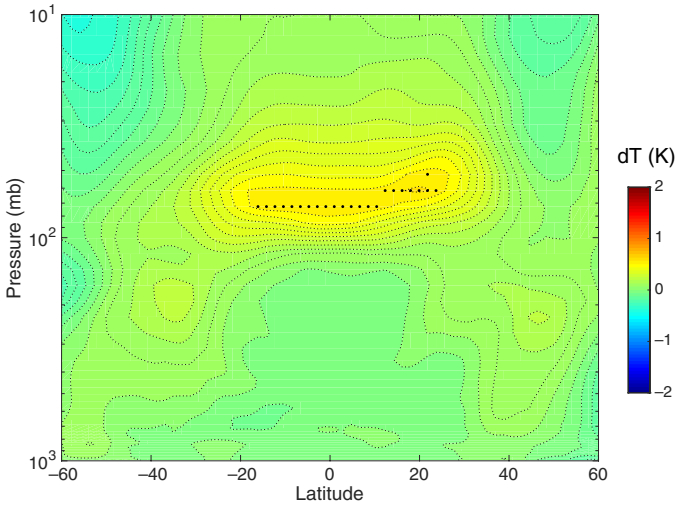

Fig. 4. Average annual temperature perturbation due to BC injection. This plot shows the difference between a control run with no BC injected and a run with 10 Gg year^{-1} of BC injected at 13.5 km at the equator; as in Fig. 3B, it is the average of 3 to 6 years from the run shown in Fig. 3A. The dots denote where the difference is greater than 1.5 times the SD of the mean. The peak values are ~0.5 K just above the tropical tropopause.

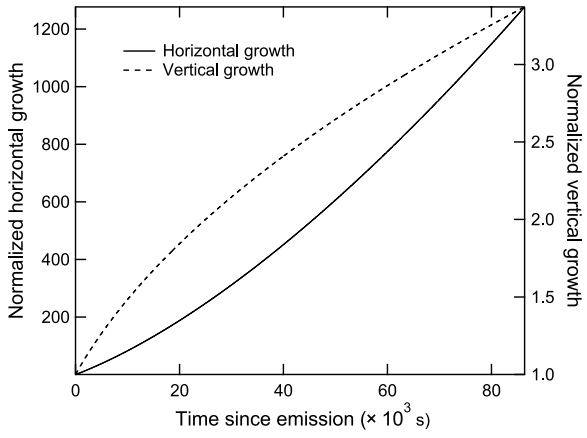

Fig. 5. Horizontal and vertical growth of a single plume. Both horizontal and vertical dimensions are normalized to the initial values and thus dimensionless.

or Russia (*32*). The additional turbulence during lofting is expected to facilitate the CIM dispersion.

Environmental considerations

Increasing the stratospheric burden of CIM via SPL will likely have unintended consequences similar to those from direct stratospheric injection. Of concern are increased stratospheric temperatures, changes in transport, the potential for stratospheric ozone depletion, and changes in surface precipitation patterns. These topics have been acknowledged and addressed in previous modeling studies of SAI (*25*). The additional environmental concern with our SPL method is the use of RAP as a lofting agent because it continues to heat the lofted air after it reaches the stratosphere.

The stratospheric burden of BC resulting from 10 Gg year^{-1} of injection in the tropics is shown in Fig. 3. Approximately 80% of the BC released rises into the stratosphere, while lofting the CIM, 10% rains out, and 10% remains in the troposphere for about a month. The effective annual increase in the global stratospheric BC burden is about 8 Gg, with most of the increase in the tropics. To place BC amounts in perspective, surface emission of BC from other sources is ~11 Tg year^{-1} (*24*), so the BC increase due to SPL is ~0.1% of the nominal annual average BC emissions. The annual average temperature response from 10 Gg year^{-1} of injection is presented in Fig. 4, which shows a peak increase of less than 1°C in the tropics where the BC concentration maximizes. A similar magnitude and pattern of heating (not shown) are produced by sulfate aerosol heating for the 1 Tg year^{-1} of SO_2 injection case. At high latitudes, stratospheric temperature changes are minimal and not statistically significant. Although the annual injection results in more than a 10-fold increase in the BC burden in the stratosphere compared to its unperturbed background state, the effective temperature change is quite small and similar to observed interannual variability, even in the tropics. If a larger amount of SO_2 is injected, then the stratospheric heating will increase, but the BC contribution will remain the same.

DISCUSSION

We have presented a novel method that makes the stratospheric CI injection substantially more practical. SPL allows CI material to be injected with the current aircraft fleet at 13.5 km as opposed to requiring platform development to inject at of 20 km. Model calculations demonstrate the potential effectiveness of SPL by showing that coinjecting small amounts of BC (10 μg m^{-3}) with CI material at 13.5 km produces an equivalent stratospheric aerosol loading to that of direct injection of the same amount of CI material at 20 km.

Global model simulations were used to quantify the impact of SPL on stratospheric temperatures. For the injection scenario used, which limited the total BC emitted to 10 Gg year^{-1}, temperature increases due to BC heating less than 1°C were calculated in the tropical lower stratosphere with minimal changes elsewhere. This change is in addition to any temperature increases due to the CIM used, in this case, SO_2. The case run for this study used 2 Tg year^{-1} of SO_2, and model results give statistically significant temperature increases maximizing at less than 2°C in the tropical lower stratosphere. For this case, injections occur over a 10-day period once per year. Stratospheric heating may be substantially reduced if light-absorbing organic aerosols, known as brown carbon (BrC) are used instead. BrC is often bleached in hours to days. After bleaching, BrC loses its light absorbing ability, and hence its impact on the temperature and circulation of the stratosphere will be much reduced (*33*, *34*).

There may be a regional cloud coverage impact associated with SPL. Convection above the injection location could be increased. The local increase in upper tropospheric BC particles could change cirrus cloud coverage by acting as ice nuclei (*35*) and heating air parcels and therefore reducing relative humidity in these air parcels. The BC particle number density in lofted air is high enough (~3000 per cm^3) that ice particles that may form will likely be small and sedimentation will be unimportant (*36*). The small amount of BC and CIM that do not enter the stratosphere could also produce cirrus changes in places surrounding the injection region. BC particles remaining in the troposphere could also perturb the local thermal structure. However, the injection region is very small (100 km by 8 km), and the period is very brief (10 days). Therefore, it is expected that the regional impacts will be limited, both spatially and temporally. Before any implementation, this must be thoroughly assessed with mesoscale and cloud-resolving model studies.

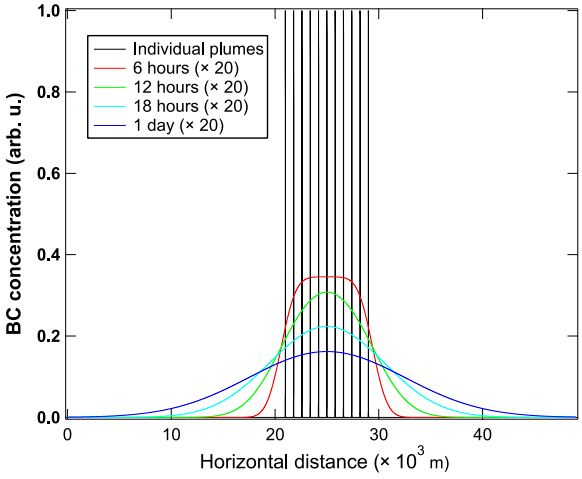

Fig. 6. Horizontal dispersion of 11 (800-m separation) plumes. All curves are in the same, albeit arbitrary, unit.

Impacts will not be restricted to the immediate vicinity of SPL injection. All BC particles (and particles from CIM) will eventually reenter the troposphere and could affect cirrus distributions globally. This effect also needs to be quantified, as do dynamical changes induced by whatever CIM is used as well. Here, we only consider the added thermal changes due to using a light-absorbing aerosol for SPL; there is much work ongoing looking at large scale weather changes due to direct stratospheric injection (*37*). Detailed modeling studies are needed to quantify this potential effect.

SPL as described here is a first step that could make it easier to initiate stratospheric CI because it does not require the development and manufacture of a new airborne platform. Before any deployment, a careful assessment of the risks and benefits is required; our analysis limits the amount of solar-absorbing aerosols, thereby minimizing potential impacts beyond that of the added stratospheric CI material. However, as noted in other studies (*5*, *8*, *25*), impacts solely from the added CI material are likely to be large. Ideally, multiple methods will be thoroughly studied theoretically to identify the optimal combination of CI implementation strategies. Such an evaluation needs to address all possibilities, including tropospheric- and stratospheric-based albedo modification methods, carbon capture, emission reductions, and adaptations. As others have also noted, CI would at best be a temporary solution, undertaken with international concurrence, to buy time by keeping surface temperature increases below critical thresholds while simultaneously developing mitigation and carbon capture technology (*4*). SPL may allow implementation of SAI with abbreviated technological development.

MATERIALS AND METHODS

Global climate model: CESM-CARMA

We use the National Science Foundation/Department of Energy CESM coupled with a sectional aerosol scheme, the CARMA (CESM-CARMA) (*24*, *38*, *39*) for this study. The horizontal resolution of the model is 1.9° (latitude) by 2.5° (longitude) with 56 vertical levels up to ~1.8 hPa. The model's time step is 30 min. The model runs with both stratospheric and tropospheric chemistry. For this study, we inject BC and CIM into one model grid box during daytime hours (8:00 a.m. to 8:00 p.m. local time) during 10 days in June over a 10-year period. The thickness of one model grid box near 13.5 km is about 1 km. The model is free running with the prescribed sea surface temperatures, and the injected aerosols are radiatively active. CARMA tracks two groups of aerosols. The first group consists of pure sulfate with 20 size bins, ranging from 0.2 nm to 1.3 μm in radius. The second group consists of internal mixtures (with the core-shell approximation) including organics, sulfate, dust, sea salt, and BC, ranging from 0.5 to 8.7 μm in radius.

CARMA provides detailed particle information (i.e., wet radius, chemical composition, and hygroscopicity), which varies with time and location. The information is used to find aerosol optical properties from a lookup table generated based on the Mie theory. Refractive indices of 1.95 + 0.79i were used for BC at mid-visible wavelengths (*19*). The calculated optical properties are then passed into CESM's radiation module (Rapid Radiative Transfer Model for GCMs) (*40*) for radiative calculations (e.g., heating rate and forcing).

The same model and similar model settings were applied to simulate the 2017 Pacific Northwest fire smoke (*19*). The observed plume lofting in the 2017 event was reproduced by CESM-CARMA with aerosol-radiation interactions. In the present study, we assume that the soot particles are spheres rather than fractal aggregates, likely representing a lower bound for the lofting efficiency because fluffy soot aggregates would absorb more sunlight, hence introducing more buoyancy. The size distribution for BC for both studies is based on a daily mean size distribution retrieved by Aerosol Robotic Network at the University of Nevada, Reno on 26 August 2013 when Rim fire smoke heavily affected the site (*41*).

Model evaluation

For the 2017 event, we used the model to simulate the plume rise with various BC-to–organic carbon ratios (BC/OC). We found that the model was able to reproduce the plume rise when BC/OC is set to 0.02. Therefore, how well the model performed can be judged by how close the assumed BC/OC ratio of 0.02 is to the real BC/OC ratio. There are a few reported measurements of the BC/OC ratio for other fire plume events in the troposphere and lower stratosphere [~0.03, (*42*), 0.015 to 0.025 (*41*), and ~0.004 (*43*)]. Because the ratio varies fire to fire, these results can only be used to bracket our model performance. The value that we use (0.02) falls within the range noted for the previously measured fires.

Model suitability

The CESM resolution is too coarse to explicitly resolve thunderstorm events that led to the overshooting pyroCB in the 2017 wildfire case or to model the detailed initial plume evolution discussed in this work. However, the goal of this work is to determine how to loft CIM from 13.5 to above 20 km. For this goal, the model is adequate, as illustrated in the 2017 pyroCb work. The reason that we are able to model a plume rising is because, in both cases, the plume is lofted by solar heating, which depends on only BC density (microgram per cubic centimeter), and is plume size independent as long as the attenuation of solar power by BC is not substantial inside the plume (true in both cases). The success of modeling the plume rise for the 2017 pyroCb event lends us high confidence that the model is adequate for SPL modeling.

Considerations of the injection

Injections of CIM in conventional scenarios are usually made year around (*25*). The SPL method, on the other hand, requires injections

to be made in much shorter period. The reason is that the total amount of RAP needed to loft a given amount of CIM is determined partially by dilution. More dilution will lead to more required RAP. To minimize dilution, the injection should as compact as possible in terms of both space and time. The 10-day period is chosen with the consideration of reasonable flights achievable per day. If the period is stretched to the entire year as in conventional scenarios, then the RAP requirement will increase substantially, mostly due to vertical dilution that can be ignored in our model experiment.

The effectiveness of SPL depends on how much solar energy a volume of air mass can absorb. More absorbed solar energy leads to more heating, which, in turn, leads to stronger lofting. As long as CIM does not impede the absorption capability of the SPL material (RAP), it does not impact the effectiveness of SPL. Therefore, it is not the ratio of RAP to SO_2 that is important for the lofting but rather the ratio of RAP to total air mass at the injection altitude.

Injection plume modeling

In this work, we adapt the Gaussian diffusion model by Dürbeck and Gerz (*28*). Under this framework, the cross-sectional growths of a single plume can be expressed analytically

$$\sigma_h(t) = \left[\frac{2}{3}s^2 D_v t^3 + s^2\sigma_{v,0}^2 t^2 + 2D_h t + \sigma_{h,0}^2\right]^{1/2} \quad (1)$$

and

$$\sigma_v(t) = \left(2D_v t + \sigma_{v,0}^2\right)^{1/2} \quad (2)$$

where h and v denote the horizontal and vertical directions, s is the wind shear rate, D is the diffusion coefficient, and $\sigma_{h,0}$ and $\sigma_{v,0}$ are the initial plume width and height, respectively.

For a single plume (a horizontally laid cylinder), the horizontal stretching and diffusion perpendicular to the cylinder are dominant factors that control the plume dispersion. The modeled plume horizontal width grows about 1200 times over 1 day (Fig. 5).

To disperse the RAP and CIM, multiple plumes are generated in very close proximity. An example is given in Fig. 6. An aircraft injects 10^5 kg of CIM on a 200-km track (a round trip in a 100-km-long box). The initial plume diameter at a 13.5-km altitude is assumed to be approximately 1.3 m, which is determined by the flight track length and the CIM load. The initial diameter determines the final combined plume width. The same amount of RAP in a larger volume will produce a smaller heating effect. Because there are uncertainties in the plume spread, as a conservative estimate, we assume that the initial plume diameter is 10 times larger or 13 m. It will take actual in-flight tests to assess the actual plume expansion and how much RAP is needed. Here, we choose conditions that likely result in an overestimate of required RAP to achieve the desired lofting. Therefore, the calculated environmental impacts from our RAP estimate are an upper limit.

A total of 11 plumes [13-m full width at half maximum (FWHM) diameter cylinders] are generated with an 800-m separation between neighboring plumes. Although, in practice, thousands of plumes will be laid each day, 11 plumes are sufficient to simulate the plume dispersion and yet allows clear illustration in Fig. 6. Individual plumes are assumed to disperse according to the Gaussian model. Because of the close proximity of plumes, these plumes quickly merge into a single plume layer of ~8.8-km horizontal FWHM after 6 hours. Adding more plumes within this 8-km band does not affect the width evolution. The combined plume continues to evolve, eventually expanding to a width of ~17.4 km after 1 day. The time-averaged plume width is ~11.4 km, so the BC concentration is diluted by about a factor of 1.4 in the first day. Therefore, if the initial BC concentration inside an 8-km wide box is set at 1.4 times the value used in Results section (~10 $\mu g\ m^{-3}$), then it is sufficient to loft the CIM material into the stratosphere. The length of the box is set at 100 km. To achieve a similar lofting as simulated in the global model of grid cell area of 208 km by 279 km, the amount of BC needed for a 10-day period is about 10 Gg for this 100 km–by–8 km area.

For a single layer of plumes laid side by side as shown in Fig. 6, additional dilution due to vertical diffusion and solar heating of BC and subsequent vertical plume raise has to be considered. This dilution is difficult to characterize without sophisticated modeling. However, in any realistic CI scenario, multiple layers of plumes will be laid in each day. Closely stacked layers of plumes will likely greatly reduce the effect of the vertical dilution.

REFERENCES AND NOTES

1. Intergovernmental Panel on Climate Change, in *Climate Change 2013: The Physical Science Basis. Contribution of Working Group I to the Fifth Assessment Report of the Intergovernmental Panel on Climate Change,* T. F. Stocker, D. Qin, G.-K. Plattner, M. Tignor, S.K. Allen, J. Boschung, A. Nauels, Y. Xia, V. Bex, P.M. Midgley, Eds. (Cambridge Univ. Press, 2013), pp. 1535.
2. Intergovernmental Panel on Climate Change, in *Global Warming of 1.5°C. An IPCC Special Report on the Impacts of Global Warming of 1.5°C Above Pre-Industrial Levels and Related Global Greenhouse Gas Emission Pathways, in the Context of Strengthening the Global Response to the Threat of Climate Change, Sustainable Development, and Efforts to Eradicate Poverty,* V. Masson-Delmotte, P. Zhai, H.-O. Pörtner, D. Roberts, J. Skea, P.R. Shukla, A. Pirani, W. Moufouma-Okia, C. Péan, R. Pidcock, S. Connors, J.B.R. Matthews, Y. Chen, X. Zhou, M.I. Gomis, E. Lonnoy, T. Maycock, M. Tignor, T. Waterfield, Eds. (IPCC, 2018), p. 661.
3. Royal Society and Royal Academy of Engineering, in *Greenhouse Gas Removal* (Royal Society, 2018), p. 134.
4. D. G. MacMartin, K. L. Ricke, D. W. Keith, Solar geoengineering as part of an overall strategy for meeting the 1.5 C Paris target. *Phil. Trans. R. Soc. A* **376**, 20160454 (2018).
5. National Research Council, in *Climate Intervention: Reflecting Sunlight to Cool Earth* (The National Academies Press, 2015), p. 276.
6. P. J. Crutzen, Albedo enhancement by stratospheric sulfur injections: A contribution to resolve a policy dilemma? *Clim. Change* **77**, 211–220 (2006).
7. T. M. L. Wigley, A combined mitigation/geoengineering approach to climate stabilization. *Science* **314**, 452–454 (2006).
8. Royal Society, in *Geoengineering the Climate: Science, Governance and Uncertainty* (Royal Society, 2009), p. 82
9. M. I. Budyko, *Climatic Changes* (American Geophysical Union., 1977), p. 261.
10. National Academy of Engineering, in *Policy Implications of Greenhouse Warming: Mitigation, Adaptation, and the Science Base* (National Academy Press, 1992), p. 944.
11. J. Latham, Control of global warming? *Nature* **347**, 339–340 (1990).
12. J. Latham, K. Bower, T. Choularton, H. Coe, P. Connolly, G. Cooper, T. Craft, J. Foster, A. Gadian, L. Galbraith, H. Iacovides, D. Johnston, B. Launder, B. Leslie, J. Meyer, A. Neukermans, B. Ormond, B. Parkes, P. Rasch, J. Rush, S. Salter, T. Stevenson, H. Wang, Q. Wang, R. Wood, Marine cloud brightening. *Philos. Trans. R. Soc.A* **370**, 4217–4262 (2012).
13. U. Lohmann, B. Gasparini, A cirrus cloud climate dial? *Science* **357**, 248–249 (2017).
14. D. L. Mitchell, W. Finnegan, Modification of cirrus clouds to reduce global warming. *Environ. Res. Lett.* **4**, 045102 (2009).
15. A. Robock, Atmospheric science: Whither geoengineering? *Science* **320**, 1166–1167 (2008).
16. S. Solomon, J. S. Daniel, R. R. Neely III, J.-P. Vernier, E. G. Dutton, L. W. Thomason, The persistently variable "background" stratospheric aerosol layer and global climate change. *Science* **333**, 866–870 (2011).
17. W. Smith, G. Wagner, Stratospheric aerosol injection tactics and costs in the first 15 years of deployment. *Environ. Res. Lett.* **13**, 12400 (2018).
18. D. W. Keith, Photophoretic levitation of engineered aerosols for geoengineering. *Proc. Natl. Acad. Sci. U.S.A.* **107**, 16428–16431 (2010).
19. P. Yu, O. B. Toon, C. G. Bardeen, Y. Zhu, K. H. Rosenlof, R. W. Portmann, T. D. Thornberry, R.-S. Gao, S. M. Davis, E. T. Wolf, J. de Gouw, D. A. Peterson, M. D. Fromm, A. Robock, Black

carbon lofts wildfire smoke high into the stratosphere to form a persistent plume. *Science* **365**, 587–590 (2019).
20. D. A. Peterson, J. R. Campbell, E. J. Hyer, M. D. Fromm, G. P. Kablick III, J. H. Cossuth, M. T. DeLand, Wildfire-driven thunderstorms cause a volcano-like stratospheric injection of smoke. *npj Clim. Atmos. Sci.* **1**, 30 (2018).
21. O. Torres, P. K. Bhartia, G. Taha, H. Jethva, S. Das, P. Colarco, N. Krotkov, A. Omar, C. Ahn, Stratospheric injection of massive smoke plume from Canadian boreal fires in 2017 as seen by DSCOVR-EPIC, CALIOP, and OMPS-LP observations. *J. Geophys. Res.* **125**, e2020JD032579 (2020).
22. B. Kravitz, A. Robock, D. T. Shindell, M. A. Miller, Sensitivity of stratospheric geoengineering with black carbon to aerosol size and altitude of injection. *J. Geophys. Res.* **117**, D09203 (2012).
23. J. Jägermeyr, A. Robock, J. Elliott, C. Müller, L. Xia, N. Khabarov, C. Folberth, E. Schmid, W. Liu, F. Zabel, S. S. Rabin, M. J. Puma, A. Heslin, J. Franke, I. Foster, S. Asseng, C. G. Bardeen, O. B. Toon, C. Rosenzweig, A regional nuclear conflict would compromise global food security. *Proc. Natl. Acad. Sci. U.S.A.* **117**, 7071–7081 (2020).
24. P. Yu, O. B. Toon, C. G. Bardeen, M. J. Mills, T. Fan, J. M. English, R. R. Neely, Evaluations of tropospheric aerosol properties simulated by the community earth system model with a sectional aerosol microphysics scheme. *J. Adv. Model. Earth Syst.* **7**, 865–914 (2015).
25. S. Tilmes, J. H. Richter, M. J. Mills, B. Kravitz, D. G. MacMartin, R. R. Garcia, D. E. Kinnison, J.-F. Lamarque, J. Tribbia, F. Vitt, Effects of different stratospheric SO_2 injection altitude on stratospheric chemistry and dynamics. *J. Geophys. Res. A.* **123**, 4654–4673 (2018).
26. S. Tilmes, J. H. Richter, B. Kravitz, D. G. Mac Martin, M. J. Mills, I. R. Simpson, A. S. Glanville, J. T. Fasullo, A. S. Phillips, J.-F. Lamarque, J. Tribbia, J. Edwards, S. Mickelson, S. Ghosh, CESM1(WACCM) stratospheric aerosol geoengineering large ensemble project. *Bull. Am. Meteorol. Soc.* **99**, 2361–2371 (2018).
27. P. Konopka, Analytical Gaussian solutions for Anisotropie diffusion in a linear shear flow. *J. Non Equilib. Thermodyn.* **20**, 79–91 (1995).
28. T. Dürbeck, T. Gerz, Dispersion of aircraft exhausts in the free atmosphere. *J. Geophys. Res.* **101**, 26007–26015 (1996).
29. U. Schumann, P. Konopka, R. Baumann, R. Busen, T. Gerz, H. Schlager, P. Schulte, H. Volkert, Estimate of diffusion parameters of aircraft exhaust plumes near the tropopause from nitric oxide and turbulence measurements. *J. Geophys. Res.* **100**, 14147–14162 (1995).
30. J. P. Smith, J. A. Dykema, D. W. Keith, Production of sulfates onboard an aircraft: Implications for the cost and feasibility of stratospheric solar geoengineering. *Earth Space Sci.* **5**, 150–162 (2018).
31. D. Visioni, D. G. MacMartin, B. Kravitz, S. Tilmes, M. J. Mills, J. H. Richter, M. P. Boudreau, Seasonal injection strategies for stratospheric aerosol geo-engineering. *Geophys. Res. Lett.* **46**, 7790–7799 (2019).
32. P. A. Newman, J. C. Wilson, M. N. Ross, C. A. Brock, P. J. Sheridan, M. R. Schoeber, L. R. Lait, T. P. Bui, M. Loewenstein, J. R. Podolske, Chance encounter with a stratospheric kerosene rocket plume from Russia over California. *Geophys. Res. Lett.* **28**, 959–962 (2001).
33. A. Laskin, J. Laskin, S. A. Nizkorodov, Chemistry of atmospheric brown carbon. *Chem. Rev.* **115**, 4335–4382 (2015).
34. S. Dansari, A. Andersson, S. Bikkina, H. Holmstrand, K. Budhavant, S. Satheesh, E. Asmi, J. Kesti, J. Backman, A. Salam, D. S. Bisht, S. Tiwari, Z. Hameed, Ö. Gustafsson, Photochemical degradation affects the light absorption of water-soluble brown carbon in the South Asian outflow. *Sci. Adv.* **5**, eaau8066 (2019).
35. Z. A. Kanji, L. A. Ladino, H. Wex, Y. Boose, M. Burkert-Kohn, D. J. Cziczo, M. Krämer, Overview of ice nucleating particles. *Meteor. Monogr.* **58**, 1.1–1.33 (2017).
36. E. Jensen, G. Diskin, R. P. Lawson, S. Lance, T. P. Bui, D. Hlavka, M. M. Gill, L. Pfister, O. B. Toon, R. Gao, Ice nucleation and dehydration in the tropical tropopause layer. *Proc. Natl. Acad. Sci. U.S.A.* **110**, 2041–2046 (2013).
37. I. R. Simpson, S. Tilmes, J. H. Richter, B. Kravitz, D. G. MacMartin, M. J. Mills, J. T. Fasullo, A. G. Pendergrass, The regional hydroclimate response to stratospheric sulfate geoengineering and the role of stratospheric heating. *J. Geophys. Res.* **124**, 12587–12616 (2019).
38. C. G. Bardeen, O. B. Too, E. J. Jensen, D. R. Marsh, V. L. Harvey, Numerical simulations of the three-dimensional distribution of meteoric dust in the mesosphere and upper stratosphere. *J. Geophys. Res.* **113**, D17202 (2008).
39. O. B. Toon, R. P. Turco, D. Westphal, R. Malone, M. Liu, A multidimensional model for aerosols—Description of computational analogs. *J. Atmos. Sci.* **45**, 2123–2144 (1988).
40. M. J. Iacono, J. S. Delamere, E. J. Mlawer, M. W. Shephard, S. A. Clough, W. D. Collins, Radiative forcing by long-lived greenhouse gases: Calculations with the AER radiative transfer models. *J. Geophys. Res.* **113**, D13103 (2008).
41. P. Yu, O. B. Toon, C. G. Bardeen, A. Bucholtz, K. H. Rosenlof, P. E. Saide, A. D. Silva, L. D. Ziemba, K. L. Thornhill, J.-L. Jimenez, P. Campuzano-Jost, J. P. Schwarz, A. E. Perring, K. D. Froyd, N. L. Wagner, M. J. Mills, J. S. Reid, Surface dimming by the 2013 Rim Fire simulated by a sectional aerosol model. *J. Geophys. Res. Atmos.* **121**, 7079–7087 (2016).
42. F. Dahlkötter, M. Gysel, D. Sauer, A. Minikin, R. Baumann, P. Seifert, A. Ansmann, M. Fromm, C. Voigt, B. Weinzierl, The Pagami Creek smoke plume after long-range transport to the upper troposphere over Europe–Aerosol properties and black carbon mixing state. *Atmos. Chem. Phys.* **14**, 6111–6137 (2014).
43. J. Ditas, N. Ma, Y. Zhang, D. Assmann, M. Neumaier, H. Riede, E. Karu, J. Williams, D. Scharffe, Q. Wang, J. Saturno, J. P. Schwarz, J. M. Katich, G. R. Mc Meeking, A. Zahn, M. Hermann, C. A. M. Brenninkmeijer, M. O. Andreae, U. Pöschl, H. Su, Y. Cheng, Strong impact of wildfires on the abundance and aging of black carbon in the lowermost stratosphere. *Proc. Natl. Acad. Sci. U.S.A.* **115**, E11595–E11603 (2018).

Acknowledgments: We thank D. W. Fahey for helpful discussions. We thank the Climate Simulation Laboratory at NCAR's Computational and Information Systems Laboratory (CSL) for computing resources (ark:/85065/d7wd3xhc). **Funding:** P.Y. was supported by the Second Tibetan Plateau Scientific Expedition and Research Program (2019QZKK0604). O.B.T. was supported, in part, by the Open Philanthropy Project. **Author contributions:** The original idea for this study was conceived by R.-S.G. and K.H.R. P.Y. performed the model simulations. All the authors contributed to developing the methodology and writing the manuscript. **Competing interests:** R.-S.G. and K.H.R. are inventors on a provisional patent application related to this work filed by the National Oceanic and Atmospheric Administration or NOAA (prov. no. 63/108633, filed 2 November 2020). The authors declare that they have no other competing interests. **Data and materials availability:** All data needed to evaluate the conclusions in the paper are present in the paper. Model simulation output used to produce the graphics is available at https://osf.io/e5jnv/?view_only=3d4dbd6726df4184bcb46f65f1f4695c, with identifier DOI: 10.17605/OSF.IO/E5JNV. Any questions regarding the data format can be addressed to P.Y.

Submitted 14 September 2020
Accepted 24 March 2021
Published 14 May 2021
10.1126/sciadv.abe3416

Citation: R.-S. Gao, K. H. Rosenlof, B. Kärcher, S. Tilmes, O. B. Toon, C. Maloney, P. Yu, Toward practical stratospheric aerosol albedo modification: Solar-powered lofting. *Sci. Adv.* **7**, eabe3416 (2021).